eJSE International

Electronic Journal of Structural Engineering (10) 2010

Experimental Nonlinear FE Modelling & Eurocode 3 Analyses of Steel Flush Endplate Joints

P.J. Fanning & M.J. Tucker
University College Dublin, Dublin, Ireland
Email: paul.fanning@ucd.ie

ABSTRACT: Structural steel joints form an integral part of all structural steel frames and regardless of the joint type employed the behaviour and response of the joints is of primary importance in determining the manner in which the frame resists both vertical and horizontal loading. An understanding of joint stiffness, strength and ductility is required. Eurocode 3 provides guidance for predicting the ultimate strength, rotational capacity and rotational stiffness of steel flush endplate joints. This paper examines in detail the correlation between Eurocode 3 predictions and actual behaviour recorded in full scale tests and validated numerical models. The detailed three dimensional finite element analysis methods used enable the significant differences to be explained by reference to the initial assumptions made in the Eurocode 3 calculations.

1 INTRODUCTION

Partial strength joints, in which the joint capacity is less than that of the connected member, have been the subject of particular attention in recent times following moderate seismic events in which the prequalified joints did not behave as anticipated, and damage to the traditional moment resisting frames was widespread (Popov et al. 1998, Mahin 1998, Mahin et al. 2002). As a result, alternative approaches to the analysis and design of frames and joints were sought to address the issue of the vulnerability of steel frames to seismic loading. One of the alternative approaches to joint design has been to allow plastic deformation to occur within the joint itself, by proportioning of the connection elements to control, rather than prevent, plastic deformations (FEMA 2000). Flush endplate joints are a particular form of partial strength, semi-rigid joints (SCI 1996, Hughes et al. 1999). These endplate joints are commonly used in frames designed for wind loading by the wind moment method, and require similar behavioural characteristics and properties as joints designed for earthquake loading, except on a smaller scale.

When modelling a structure at global level, regardless of the joint type, the joint properties required for analysis can be determined by a variety of means. Accepting that large scale experimental testing is not practical, the use of semi empirical rules based on testing and/or simplified behavioural or finite element models offer the most amenable options. This paper aims to compare and contrast two such options, namely, the design method as proposed in Eurocode 3 (Eurocode 3) and the results of analytical models which have been validated against a series of experimental tests. In describing the numerical modeling particular attention is paid to the aspects of the modelling approach adopted with reference to the elements and associated mesh employed, the non-linear material data used, contact representation and the numerical simulation of plasticity. The models constructed are shown to accurately capture the experimentally recorded global deformations, strains and projected failure modes. Finally the results of the finite element models are compared with the design guidelines outlined in Eurocode 3, with particular reference to predicted joint properties, joint classification, bolt forces and yield patterns.

2 JOINTS TESTED

The joints studied in this paper are three of a set of joints tested at Trinity College Dublin (Thomson 2001). A schematic of the support, loading arrangements and connection details, common to the three tests, is shown in Figure 1; locations of strain gauges and LVDT's used for comparison with FE results are also included. For each joint tested the overall height and length of the test configuration, along with the bolt spacing, bolt size and beam positioning on the endplate were constant.

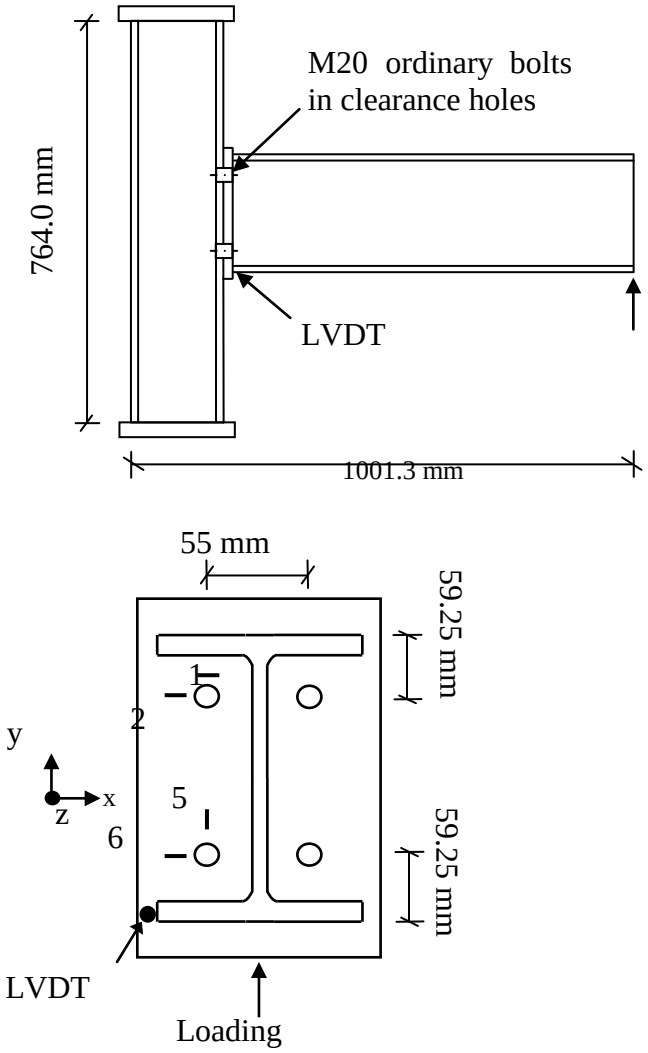

Figure 1. Schematic, LVDT and Strain Gauge Locations

Joints were loaded monotonically under displacement control to the maximum stroke of 50mm available at load actuator. The three test joints varied in endplate thickness, t_{ep}, column sizes and bolt grade only. Grade S275 steel sections were used throughout. The component sizes for each of the three tests labelled Joints J1, J2 and J3 respectively are tabulated in Table 1. All three joints tested consisted of a 254 × 146 × 37 UB section. Otherwise, Joint J1 consisted of a 203 × 203 × 86 UC section, a 10 mm thick endplate and M20 grade 8.8 bolts. Joint J3 differed from Joint J1 only in increased endplate thickness and bolt grade. Joint J2 consisted of a lighter column section, than the other two joints, namely a 203 × 203 × 52 UC, a 12 mm thick endplate and M20 grade 8.8 bolts.

The joints are variations of the wind moment connections described in [5] and were each designed for a particular mode of failure in accordance with Eurocode 3. Joints J1 and J3 were designed to fail due to plastic deformation of the endplate, a mode 1 failure. Relative to Joint J1, Joint J2 had a thicker endplate and lighter column section with the objective of achieving a mode 2 failure, consisting of column flange and bolt yielding. In each joint bolts were hand tightened and hence no prestress was induced.

Table 1. Flush Endplate Joint Details

Joint	t_{ep} mm	Column	Beam	Bolts
J1	10	203UC 86	245×146UB 37	M20, 8.8
J2	12	203UC 52	245×146UB 37	M20, 8.8
J3	12	203UC 86	245×146UB 37	M20, 10.9

3 FINITE ELEMENT MODELLING OF JOINT BEHAVIOUR

The response of a joint under loading, monotonic or cyclic, is complex with the possibility of local buckling of the beam and column web and flanges, the development of plastic deformation in the connection components, bolt failure and the separation of the various contacting surfaces in the connection.

3.1 *Solid Modelling*

In this study the ANSYS suite of finite element software was employed. Three dimensional SOLID186 elements, higher order twenty node isoparametric elements with large strain and plasticity capabilities, were used to model the beam members, column members, endplates, bolt shafts and bolt heads and nuts. These elements use a uniform reduced integration formulation which eliminates the potential for both shear and volumetric locking (i.e overly stiff behaviour). Whilst there are simpler modeling approaches available these often restrict accurate simulation of the joint behaviour. Sherbourne and Bahaari (1994) and Bahaari and Sherbourne (1996) observed difficulty in predicting the joint behaviour in the non-linear range as a result of excluding through thickness effects when using shell elements. Equally, use of link elements to model bolts led to difficulty in predicting behaviour at the ultimate load due to the lack of bending resistance in these link elements (Bahaari and Sherbourne 2000, Bose et al. 1997, Bose et al. 1996).

Advantage was taken of the symmetry of the test configurations and the mesh density, Figure 2, was chosen so that a balance was achieved between solution accuracy and demand on computer resources. Areas within the joint model, particularly around the connection elements, were meshed using a fine mesh. Welds were not modelled explicitly but continuity of mesh was ensured along all weld lines. The shafts of the bolts were assigned a diameter con-

sistent with the effective tensile area of the bolts. For M20 bolts with a tensile area of 245 mm^2, a bolt diameter of 17.66 mm was specified. The heads and nuts were modelled as circular, with diameter and depth as recommended by the Steel Construction Institute (SCI 1995). No prestressing was included for the bolts – for hand tightened bolts the effect of prestress has been shown to be negligible on the ultimate capacity if endplate bending is the predominant failure mode (Bahaari and Sherbourne 1996, Butterworth 2000). Similarly, even for joints governed by bolt failure, the joint stiffness is only effected if the preload is 40% to 60% of the bolt yield stress (Thomson 2001).

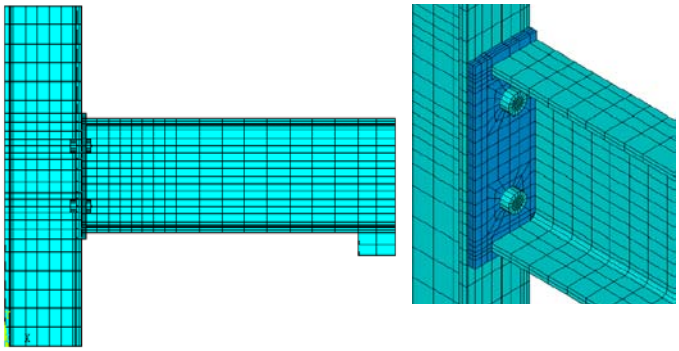

Figure 2: Typical FE Mesh

3.2 *Contact Interfaces*

Depending on the relative stiffness and strength of the various joint components, a consequence of joint deformation is the separation of adjoining surfaces, the development of high localised stresses at the area of contact between surfaces, frictional forces, or even slip of the adjoining surfaces relative to each other. To model the interaction of the contacting surfaces, 3-D CONTA174 contact elements and TARGE170 target elements were overlaid on the finite element mesh between the following interacting surfaces: the column flange and endplate; the endplate and bolt heads; the column flange and bolt nuts; the bolt shafts and bolt holes. In modelling contact, one surface is defined explicitly as the target surface and meshed with target elements while the other surface is explicitly defined as the contact surface and meshed with contact elements. Target elements are overlaid on the stiffer surface and the contact algorithm is designed to prevent penetration of the target mesh by the contact mesh. However if the stiffness of the target and contact surfaces is not so readily distinguished bi-directional penetration can be invoked – this so called "Symmetrical Contact" was found to be most appropriate for modelling these joint configurations. Parametric studies undertaken by Tucker (2005), using the ANSYS penalty based contact algorithm, identified a contact stiffness factor of 1.0 assigned for under the bolt heads and nuts and 0.1 on all other contact surfaces. In the numerical model the resulting hertzian contact stiffness, which is calculated as the product of the Young's modulus of the underlying material, the assigned contact stiffness factor and the depth of the underlying element, equated to approximately 3500kN/mm under the bolt heads and nuts and 82kN/mm on all other contact interfaces. Finally the resistance to shear forces developed by frictional stresses is also accounted for using these surface to surface contact elements by assigning a coefficient of friction of 0.3 to all mating surfaces. The maximum frictional stress beyond which sliding can occur is limited to the coefficient of friction times the contact surface pressure.

3.3 *Nonlinear Material Modelling*

The material data for the endplate, beam and column sections were obtained from uniaxial tests, in accordance with BS10002 (1990) on samples cut from the tested joints. Particular care was taken to ensure material test samples were taken from areas of the joint with limited deformation. The orientation of the samples was also considered and chosen so that they would be loaded in tension in the direction coincident with the principal loading direction in the full joint tests. The numerical simulations are executed using large deflection and large strain analysis theory and hence the nonlinear material curve is defined in true stress and true strain format. The component test data and the true stress vs. true strain curve used in the models are shown in Tables 2 (a), (b) and Figure 3 respectively. Young's Modulus and poisons ratio were taken as 205,000 N/mm^2 and 0.3 respectively for all components.

In modelling plasticity, the point at which material yielding begins is identified, yield criterion, and how the material behaves post yield is specified, flow and hardening rules. The specimens tested to obtain the material data were subjected to a uniaxial stress state while the joint components are subjected to multi-axial stress states during their working life. The yield criteria is any descriptive statement that defines the condition under which yielding will occur (Boresi et al. 1993). Using ANSYS the yield criterion is met when the Von-Mises equivalent stress at an integration point reaches a predefined value, taken as the uniaxial yield stress identified in material sample tests. The flow rule relates the increments of plastic strain to the increments of plastic stress and how the plastic strain components develop after

yielding. For the joint components the flow rule chosen was associative. This implies that the plastic strains develop in a direction normal to the yield surface. ANSYS offers two hardening rules that can be associated with the post-yield flow rule, either Isotropic Hardening or Kinematic Hardening. These Hardening rules define the nature of any subsequent yielding in the material by predicting how the yield surface will change during plastic flow. Isotropic Hardening assumes uniform expansion of the yield surface during plastic flow while Kinematic Hardening assumes that the yield surface shifts in stress space during plastic flow, and thereby includes the Bauschinger effect. For joints loaded monotonically, the use of either hardening rule is appropriate, as only the stresses and strains upon load reversal are affected by the chosen hardening rule.

Table 2(a). Material Data for Bolts

Point	Stress N/mm^2	Strain N/mm^2	Stress N/mm^2	Strain N/mm^2
1	604.20	0.00295	917.64	0.00437
2	670.20	0.12	1040.00	0.048
3	670.20	0.20	1040.00	0.20

Table 2(b). Material Data for Endplate Column and Beam Sections

Point	True Stress N/mm^2	True Strain N/mm^2
1	287.10	0.0014
2	316.81	0.015
3	413.13	0.05
4	476.10	0.10
5	511.75	0.155

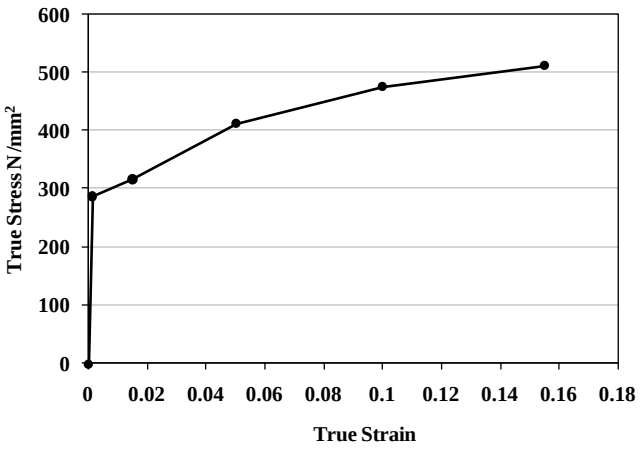

Figure 3: Assigned Beam, Column and Endplate Material Curve

3.4 *Loading & Boundary Conditions*

The models were loaded by applying an incremental displacement at the load point. Node points at either end of the column section were fixed in position for the duration of the analyses. To account for the geometrical changes and stresses induced in the elements, large deflection effects were invoked. At each increment the stiffness matrices of individual elements, and hence the global stiffness matrix, were updated and force equilibrium was ensured, at each increments, by using a force convergence criteria through a series of Newton-Raphson iterations. In total, approximately 60 displacement increments were specified for each load scenario.

4 COMPARISON OF FE & TEST RESULTS

The primary contributor to the joint deformation, in both the simulations and tests, was found to be the flexibility of the endplate. Figure 4 illustrates the experimental and analytical deformed shape of the Joint J1 and it is evident that the general deformation behaviour of the endplate was predicted well by the finite element model of the joint shown.

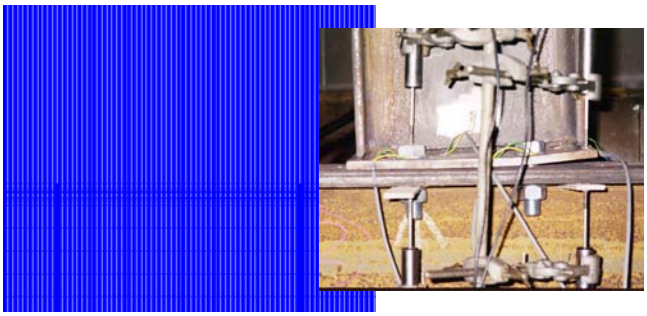

Figure 4. Deformed Shape Comparison Joint J1

The endplate, initially flush with the column flange, bends and separates from the column flange as the load on the joint increases, the separation occurring primarily along the line of the beam web and along the end and side edges of the endplate. As the load is not applied uniformly across the width of the endplate and due to the flexibility of the endplate and restraint provide by the bolt head, the corner of the endplate tends to twist inwards at higher loads.

This consistency of prediction was consistent across the three joints modelled. In the proceeding paragraphs, the effectiveness of the numerical modelling approach is demonstrated by comparison of predicted deflection and strain values with measured data sets for Joint J1 only. Tucker (2005) includes a complete discussion of the comparisons for Joints J2 and J3.

The measured and predicted deflections, at the LVDT displacement transducer positioned on the outer face of the endplate adjacent to the beam tension flange (see Figure 1) are plotted in Figure 5. While the measured data is limited by maximum

available LVDT travel, the maximum load indicated in the plot, 64 kN, corresponds closely to the maximum load applied in the experimental test.

Strain comparisons in the tension region of the endplate were obtained from Gauge 5 and Gauge 6 (see Figure 1) and are plotted in Figure 6. For Gauge 5 the finite element model predicts the behaviour accurately up to the load, 40kN, at which experimental data becomes erratic and no longer captures data consistent with the developing mode of deformation during the test. Similarly predicted strains at the location of Gauge 6 show good correlation with the experimental results.

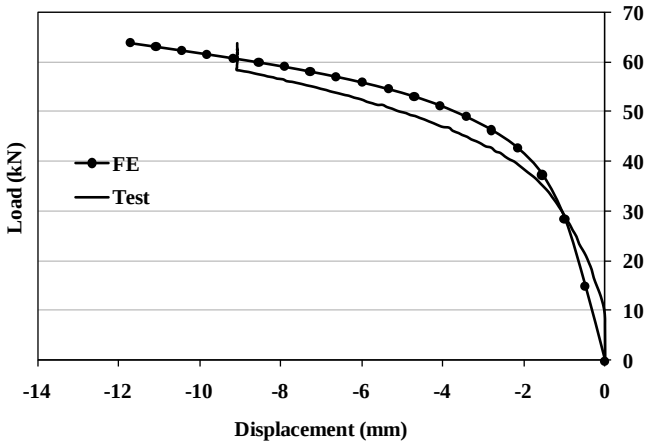

Figure 5. LVDT Load vs. Displacement for Joint J1

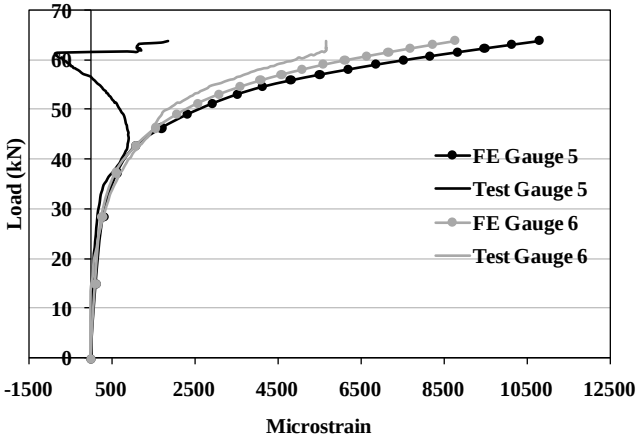

Figure 6: Load vs. Microstrain: Gauges 5 and 6

In the compression region of the endplate (Gauges 1 and 2 in Figure 1) comparisons of strain measurements are equally consistent, Figure 7. Significantly the response at Gauges 2, whereby the initial positive strain reading is followed by a two further successive strain reversals, is captured although it is noted that prior to a load of approximately 50kN, the magnitude of strains predicted by the finite element analysis are less than those measured obtained in the test. However as the level of strain develops and plastic deformation ensues the correlation between measured and predicted strains is excellent and allows for sound prediction of the ultimate joint capacity using the finite element model.

Post test examination of the joint revealed the developing mode of failure for Joint J1 to be due to plastic deformation of the endplate, or a mode 1 failure as per the Eurocode 3 definition. This was characterised by plastic response having occurred in the endplate in circular patterns around the bolt hole in the tension region and along the line of the beam web (Thomson 2001).

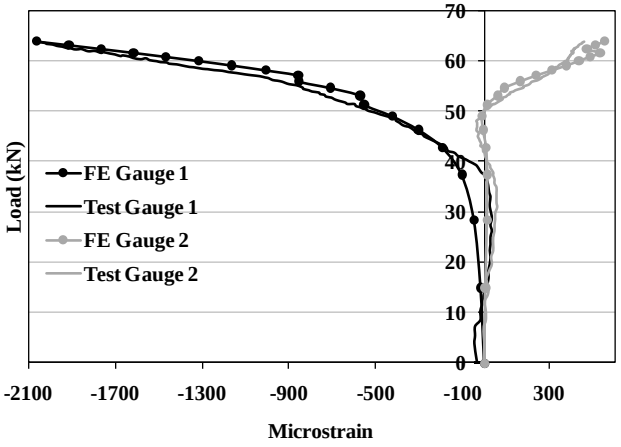

Figure 7: Load vs. Microstrain: Gauges 1 and 2

In the analytical model, accumulated equivalent plastic strain contours plotted at a load of 64kN, Figure 8, identify locations and magnitude of the plastic strains. Plastic deformation is limited primarily to the endplate. Consistent with the tests there is a zone of plastic deformation located around the tension bolt head. The FE model also predicts that this plastic zone extends up the endplate at the beam web interface.

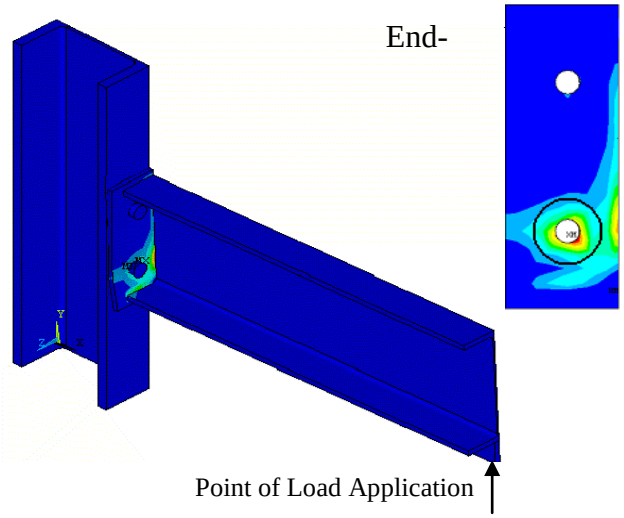

Figure 8. FE Model Plastic Strains at Ultimate Load: Joint J1

The development of tension forces in the bolts is plotted in Figure 9, the maximum bolt force is attained in the tension zone (row 1) bolts and equates to approximately 80% of the bolt yield force (148kN). It is interesting to note that the bolts in the compression zone (row 2) also develop significant tension, 47% of the yield force, as the joint deforms plastically. Therefore neither bolt rows reach yield, and the FE model identifies plastic deformation of the endplate, a mode 1 failure, as the developing failure mode – an observation which is consistent with the experimental test.

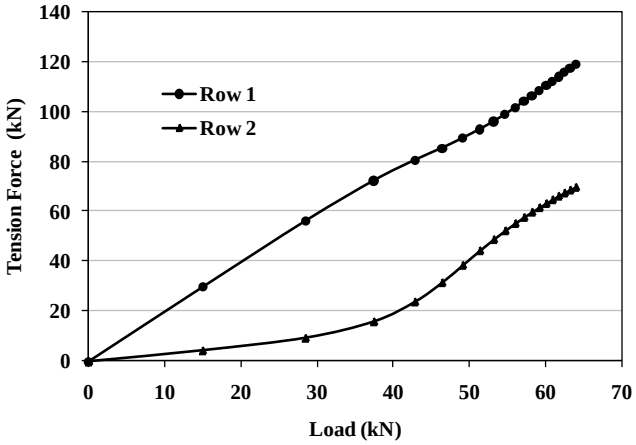

Figure 9: Tension Force per Bolt vs. Load: Joint J1

For Joint J1 an initial stiffness was determined from the slope of the linear portion of the applied load versus load point displacement response, Figure 10. The FE model predicted that the model becomes nonlinear at an applied load of 28kN which corresponded to the load at which plastic response is initiated in the endplate.

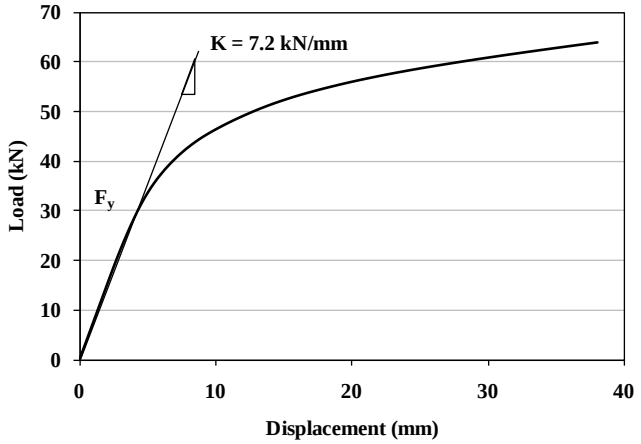

Figure 10: Load vs. Displacement at load point for Joint J1

The FE predictions for stiffness, yield and ultimate load capacity and yield and ultimate rotation capacity are summarized in Table 4 (a) to (c) for each of the joints. The load lever arm, taken as the distance between the loading point and the centre of the endplate, was used to convert load and deflection to moment and rotation for comparison with EC3.

5 EC3 ANALYSIS OF JOINTS

On the basis that all joints must be capable of transferring the full magnitude of the shear forces at a connection, joint behaviour is represented by their moment-rotation response. The relevant properties which define this response and form the basis of the various classification systems are the initial rotational stiffness, the moment resistance/ moment capacity and the rotational capacity. The basis of the component method for joint analysis adopted in Eurocode 3 is to identify the individual joint components, assess their strength and then combine these relevant components together, incorporating any interaction. In determining the moment capacity of the joint, the applied bending moment is considered as a couple, with equal and opposite tensile and compressive forces acting at the centres of tension and compression respectively.

In the tension zone of the joint, the Eurocode uses the concept of an equivalent T-stub to model the interaction between the column flange, endplate and the bolts, Figure 11.

The complex patterns of yield lines that develop in the tension region of the connection are incorporated into the analysis by an effective length, l_{eff}, of the equivalent T-stub designed to represent the length of plastic zone of the joint under loading. Depending on the relative size and strength of the endplate/column flange and bolt assembly there are three possible failure modes for the equivalent T-stub, under tension, from which the lowest is deemed to be the tension resistance of the assembly. The three possible modes of failure, Figure 11, are yielding of the column flange or endplate *(Mode 1 Failure)*, bolt failure with column flange or endplate yielding *(Mode 2 Failure)* and bolt failure alone *(Mode 3 Failure)*. For an endplate joint this T-stub tension resistance is the tensile component of the bending moment carried by bolts in the tension zone. Coupled with the compressive force acting at the centre of rotation, assumed to occur at the mid depth of the bottom beam flange, the moment capacity of the joint can be determined.

In predicting the rotational stiffness of endplate joints, Eurocode 3 also uses the component method. Each component contributing to the rotational deformation of the joint is modelled as a spring and

assigned a stiffness coefficient. By combining the component springs into a spring model, the rotational stiffness can be determined. The Eurocode provides details on the relevant components contributing to the rotational stiffness for different joint types and the formulae for determining the relevant stiffness coefficients and overall rotational stiffness of the joint.

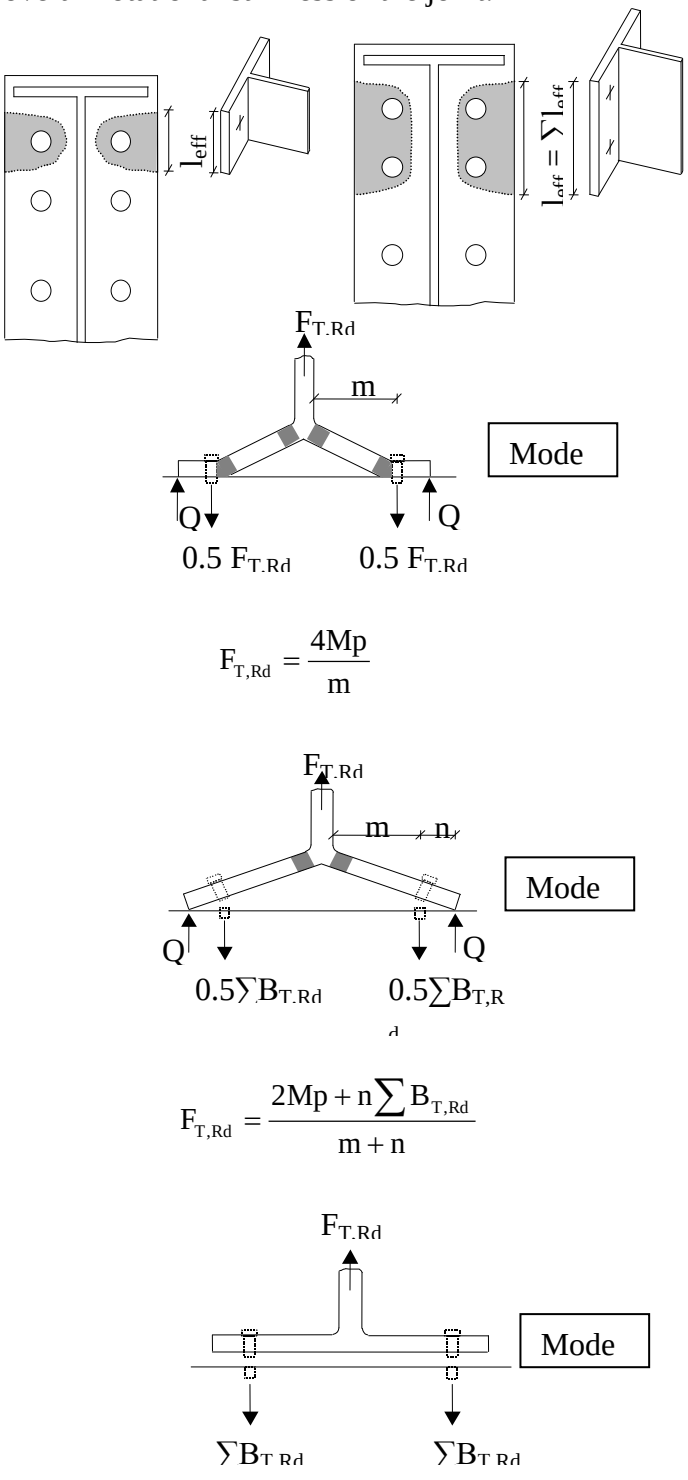

Figure 11. Eurocode 3 Equivalent T-Stub Model

Based on Eurocode 3, the dimensions and values required for the T-stub models of Joints J1, J2 and J3, are summarised in Table 3.

Table 3. Eurocode 3 Joint Parameters

Joint	Parameters m	n	∑B	Leff	Mp
	(mm)	(mm)	(kN)	(mm)	(kNm)
J1	30.49	38.11	295.56	191.55	1.37
J2	32.84	41.05	295.56	172.52	1.94
J3	30.49	26.8	458.64	191.55	1.98

6 COMPARISON OF FE & EC3 PROJECTIONS

Calculated joint properties for both FE and Eurocode 3 analyses are summarised in Table 4. For each of the three joints the assessment of the yield moment is consistent. Typically EC3 predicts a slightly higher yield moment with the maximum difference of +14% occurring for Joint J2. Initial rotational stiffnesses do not compare favourably. Across the three joints the Eurocode 3 predictions are up to 2.4 times those predicted by the FE models – this is a significant difference particularly as the FE models have been shown to capture the test response of these joints accurately. The ultimate moment capacities of the three joints are consistently underestimated by Eurocode 3, being 65%, 77% and 82% of the values predicted for Joints J1, J2 and J3 respectively using the FE models.

Table 4(a). Joint Properties Joint J1– FE vs. EC3

Joint Properties	Joint J1 FE	EC3
Initial Stiffness (kNm/rad)	4438.20	10707.43
Yield Rotation (rad)	0.005	0.0025
Yield Moment (kNm)	22.68	23.04
Ultimate Rotation (rad)	0.05	0.0097
Ultimate Moment (kNm)	53.29	34.64

Table 4(b). Joint Properties Joint J2– FE vs. EC3

Joint Properties	Joint J2 FE	EC3
Initial Stiffness (kNm/rad)	3200.00	7527.95
Yield Rotation (rad)	0.0075	0.0036
Yield Moment (kNm)	24.00	27.45
Ultimate Rotation (rad)	0.034	0.017
Ultimate Moment (kNm)	53.78	41.59

Table 4(c). Joint Properties Joint J3– FE vs. EC3

Joint Properties	Joint J3 FE	EC3
Initial Stiffness (kNm/rad)	4740.74	11872.02
Yield Rotation (rad)	0.0068	0.0028
Yield Moment (kNm)	32.00	33.18
Ultimate Rotation (rad)	0.027	0.0126
Ultimate Moment (kNm)	60.8	49.89

These comparisons have important implications for the consideration of joint contributions to overall frame behaviour. Based on the joint classification system proposed by the Eurocode, the FE determined properties would result in Joint J1 being classified as pinned, for initial stiffness classification, and partial strength for strength classification while the values predicted using the Eurocode component method would result in the same joint configuration being classed as semi-rigid for initial stiffness and nominally pinned/partial strength for strength classification. Using the FE model results Joint J3 would be classed as pinned, for initial stiffness classification, and partial strength, for strength classification, but semi-rigid and partial strength using the Eurocode component method. Both methods classify Joint J2 as pinned for initial stiffness classification, and partial strength for strength classification.

7 DISCUSSION

For the three joints, the tests, and the finite element models which correlated well with them, predicted a joint response with a higher moment capacity, greater flexibility and increased rotational ductility compared to Eurocode 3 projections. The 3D finite element models allow a thorough analysis of the complex behaviour of the moment-rotation response of flush end plate joints under loading. True contact, and separation of contact interfaces, can be accounted for as well as the progressive generation of plastic deformation zones through the use of nonlinear material models and the robust modelling procedure described above has been shown to faithfully capture the experimental response of this joint type.

Eurocode 3 proposes relatively simple rules, centred on a component type analysis of the joint, to address these complex issues – by necessity a number of assumptions are made. These assumptions explain in part the resulting differences in joint properties and ultimately the differing resulting joint classifications. The T-stub models in Eurocode 3 are sized on the basis of an effective length value, leff, Figure 11.

The distribution of plastic strain in the endplate at ultimate moment capacity for J1 is shown in Figure 8 – the solid black line indicates the circular yield zone assumed by Eurocode 3, based on joint dimensions, in its calculations. The zone of plastic deformation is far more extensive than assumed and significantly not only forms a circular pattern around the tension bolt holes but also extends up the endplate and the beam web interface. The less extensive distribution of the plastic strains assumed by EC3 calculations leads to an increased assessment of the stiffness of the endplate and hence the joint as a whole. This overestimate of joint stiffness leads subsequently to an underestimate of rotational capacity.

The Eurocode method further assumes that only the bolt row on the 'obviously' tension side of the joint contributes to the moment capacity of the joint. The bolt force distributions for J1, see Figure 9, shown that after the initiation of plastic deformation (at approximately 28kN of applied load) the tensile force in the lower bolt row develops rapidly as the plastic region extends and spreads up the endplate. This development of tensile forces in the nominally 'compressive' bolt row is not considered at all in the Eurocode. The resulting bolt row force distributions for the FE models and the Eurocode predictions, Figure 12, then explain the enhanced moment capacity observed in the tests and FE models relative to the Eurocode. It is worth noting that accounting for this tension force will also effect the bolt shear capacity calculation in accordance with the Eurocode.

8 CONCLUSIONS

In this paper, robust non-linear three-dimensional numerical modelling strategies, to simulate the response of flush endplate joint details, have been described. The models which account for component separation through the use of contact interfaces and material plasticity through the inclusion of nonlinear true-stress versus true-strain data have been shown to accurately capture measured joint behaviour for the three joints tested.

The Eurocode 3 approach was found to reliably predict the moment at which plastic response is initiated in all three joints. However the evaluation of joint stiffness was found to be inadequate with predictions being up to 2.4 times higher than those recorded in tests and FE models. Beyond the point of development of plastic deformations in the endplate the assumption that the bolt row on the nominally 'compression' side of the joint carries no tensile force is no longer valid and explains the lower value for ultimate moment capacity predicted by the Eurocode. The combined effect of overestimating initial stiffness and underestimating ultimate capacity led to two of the three joints tested being miss-classified in terms of joint behaviour.

Three dimensional FE models, despite their complexity, have been shown to be required to, and do, adequately predict the behaviour of flush endplate joints. Attempts to use simplified component type approaches, as provided in Eurocode 3, can lead to the miss-classification of joints and thereby the inappropriate distribution of forces and moments in

structural frameworks of which they form part. In the context of resolving the anomalous results predicted by Eurocode 3 further research is required to identify the extent of more appropriate sub-component models that will enable simple and reliable assessment of joint behavior.

9 ACKNOWLEDGEMENTS

The authors wish to thank Professor Brian Broderick, Trinity College Dublin and Dr. Andrew Thomson, former research student, Trinity College Dublin, for providing the experimental results for comparison with the analytical models.

REFERENCES

Bahaari, M. R. & Sherbourne, A. N., "Structural Behaviour of Endplate Bolted Connections to Stiffened Columns", *ASCE Journal of Structural Engineering*, Vol. 122, No. 8, Aug. 1996, pp. 926–935.

Bahaari, M. R. & Sherbourne, A. N., "Behaviour of Eight-Bolt Large Capacity Endplate Connections", *Computers and Structures*, Vol. 77, No. 3, 2000, pp. 315–325.

Boresi, A. P., Schmidt, R. J. & Sidebottom, O. M., "Advanced Mechanics of Materials", 5th edition, *John Wiley & Sons Inc*., USA, 1993

Bose, B., Sarkar, S. & Bahrami, M., "Extended Endplate Connections: Comparison between Three-Dimensional Nonlinear Finite Element Analysis and Full-Scale Destructive Tests", *Structural Engineering Review*, Vol. 8, No. 4, 1996, pp. 315–328.

Bose, B., Wang, Z. M. & Sarkar, S., "Finite Element Analysis of Unstiffened Flush Endplate Bolted Joints", *ASCE Journal of Structural Engineering*, Vol. 123, No. 12, Dec.1997, pp. 1614–1621.

BS10002: Part 1 "Tensile Testing of Metallic Materials: Method of Test at Ambient Temperature", *British Standards Institution (BSI)*, London, England, 1990.

Butterworth, J. W., "Bolt Force Distribution in Structural Steelwork Extended Endplate Beam to Column Connections" *PhD Thesis*, Division of Civil Engineering and Building, Schools of Science and Technology, University of Teeside, UK, 2000

Eurocode 3, "Design of Steel Structures Part 1-8: Design of Joints'", *European Committee for Standardisation (CEN)*, BS EN 1993-1-8:2005.

'FEMA-350 Recommended Seismic Design Criteria for New Steel Moment-Frame Buildings', *SAC Joint Venture*, June, 2000.

Hughes, A. F., Brown, N., D., & Anderson, D., "A Fresh Look at the Wind Moment Method", *The Structural Engineer*, Vol. 77, No. 16, Aug. 1996, pp. 22-27.

Mahin, S. A., "Lessons from Damage to Steel Buildings during the Northridge Earthquake", *Engineering Structures*, Vol. 20, Nos. 4–6, 1998, pp. 261-270.

Mahin, S. A., Malley, J. & Hamburger, R., "Overview of the FEMA/SAC Program for Reduction of Earthquake Hazards in Steel Moment Frame Structures", *Journal of Constructional Steel Research*, Vol. 58, 2002 pp. 511-528.

Popov, E. P., Yang, T.-S. & Chang, S.-P., "Design of Steel MRF Connections before and after 1994 Northridge Earthquake", Engineering Structures, Vol. 20, No. 12, 1998, pp. 1030–1038.

Steel Construction Institute, "Joints in Steel Construction–Moment Connections", *Steel Construction Institute*, Ascot, England,1995.

Sherbourne, A. N. & Bahaari, M. R., "3-D Simulation of Endplate Bolted Connections", *ASCE Journal of Structural Engineering*, Vol. 120, No. 11, Nov.1994, pp. 3122–3136.

Thomson, A. W., "The Earthquake Resistance of Flush Endplate Joints", *PhD Thesis*, Department of Civil, Structural and Environmental Engineering, Trinity College Dublin, Ireland, 2001.

Tucker, M. J., "Non-Linear Modelling of Partial Strength Steel Endplate Joints and The Inherent Seismic Resistance of Unbraced Frames", *PhD Thesis*, Department of Civil Engineering, University College Dublin, Ireland, 2005.